Thermoelectric and thermospin properties of gapped Dirac materials

Sergei G. Sharapov

ICTP, Trieste, Italy, 11-15 March, 2019

Bogolyubov Institute for Theoretical Physics
of the National Academy of Sciences of Ukraine

Conference on Modern Concepts and New Materials for Thermoelectricity

In collaboration with: V.P. Gusynin, A.A. Varlamov

Outline

1. Thermoelectric power in gapped graphene
2. Nernst - Ettingshausen effect in graphene
3. Spin Nernst (SN) effect in silicene
4. Modified Kubo formula

Thermoelectric power in gapped graphene

Thermoelectric power in gapped monolayer graphene

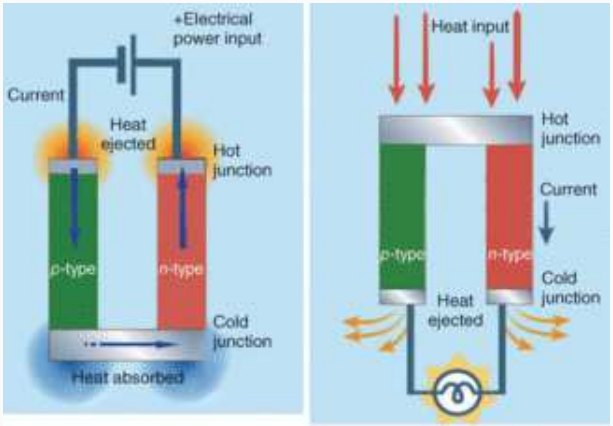

$$V = (S_B - S_A)(T_2 - T_1)$$
$$S = -\frac{\Delta V}{\Delta T} = \frac{E}{\nabla T}$$

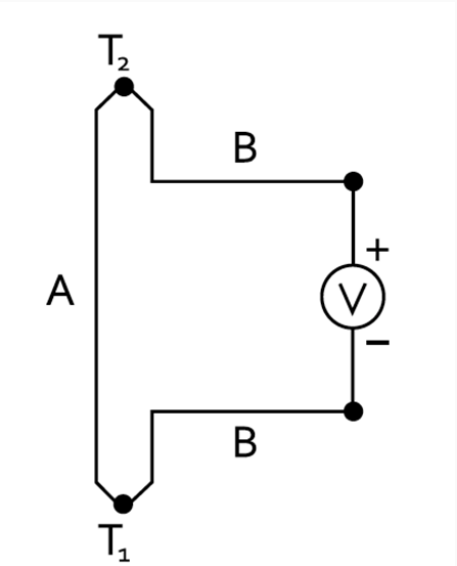

Nowdays we call this Seebeck effect. See a review C. Goupil, H. Ouerdane, K. Zabrocki, W. Seifert, N.F. Hinsche, and E. Müller, "Thermodynamics and Thermoelectricity":

Aepinus (1762), Galvani, Volta (1786) $\Rightarrow$ Ritter (1801), Schweigger (1810), Seebeck (1821)$\Rightarrow$ Peltier (1834), Thomson (1851)

Large thermoelectric effect in graphene

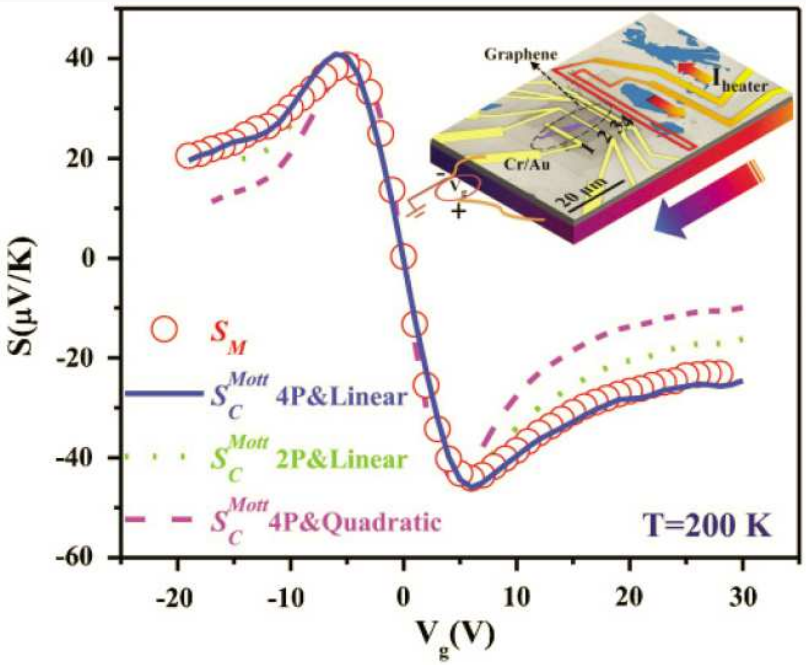

FIG. 1. (Color online) Comparison of experimentally measured Seebeck coefficient S_M (open circles) and three Seebeck curves S_C^{Mott} calculated from measured electrical conductivity using the Mott relation. The solid line is calculated with the 4P resistivity and a linear dispersion relation; the dotted line is with the two-point (2P) resistivity and a linear dispersion relation; and the dashed line is with the 4P resistivity and a quadratic dispersion relation. μ_c of this device is $\sim$1500 cm^2/Vs. The inset shows a false colored scanning electron microscopy image.

Wang, Shi, PRB 83, 113403 (11).

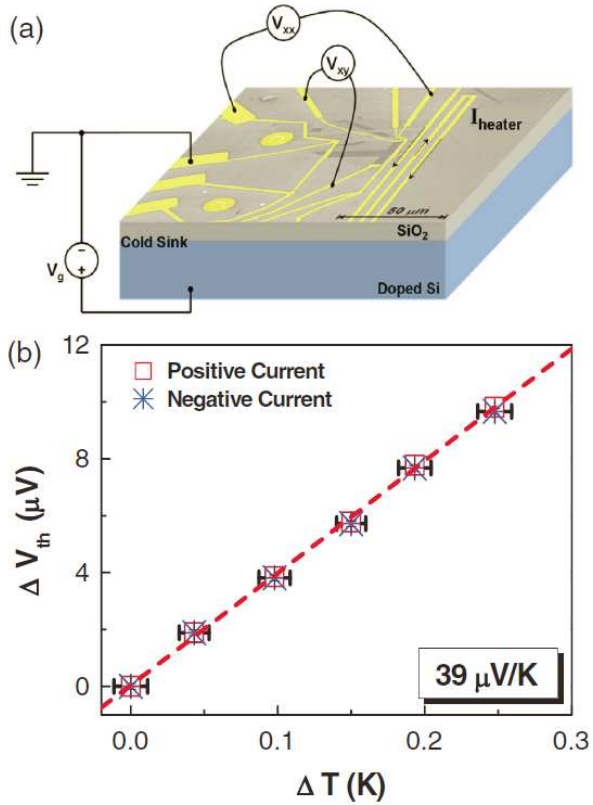

FIG. 1 (color). (a) SEM image and circuit schematic of a graphene device for thermoelectric measurements. (b) ΔT vs thermovoltage change ΔV_{th} for a series of heater power steps at 255 K and zero gate voltage. The linear fit of this curve gives the thermopower of 39 μV/K.

Wei *et al.*, PRL 102, 166808 (09).

Heat and electric transport equations

Electric field **E** and temperature gradient ∇T result in electric and heat currents.

$$\begin{cases} \mathbf{j} &= \hat{\sigma}\mathbf{E} - \hat{\beta}\nabla T, \\ \mathbf{q} &= \hat{\gamma}\mathbf{E} + \hat{\zeta}\nabla T, \end{cases}$$

It is easier to control **j** rather than **E**, express via **j**.

$$\begin{cases} \mathbf{E} &= \hat{\rho}\mathbf{j} + \hat{S}\nabla T, \\ \mathbf{q} &= \hat{\Pi}\mathbf{j} - \hat{\kappa}\nabla T, \end{cases}$$

Onsager relation: $\hat{\gamma} = \hat{\beta} T$

Only the diagonal transport is considered in the first part!

Seebeck coefficient:

$$S \equiv S_{xx} = -\frac{\beta}{\sigma} \equiv -\frac{\beta_{xx}}{\sigma_{xx}}$$

Peltier coefficient:

$$\Pi = \frac{\gamma}{\sigma} = ST$$

Approximate Mott's formula:

$$\beta = \frac{\pi^2}{3}\frac{k_B^2 T}{e}\frac{\partial \sigma}{\partial \mu} \quad \Longrightarrow \quad S = -\frac{\pi^2}{3}\frac{k_B^2 T}{e}\frac{\partial \ln \sigma}{\partial \mu}$$

Notice that $k_B/e \approx 86 \mu V/K$ close to observed in graphene which is much larger than in metals.

Odd- and evenness of transport coefficients

$$\sigma = \frac{e^2}{3}\int_{-\infty}^{\infty} d\epsilon[-n_F'(\epsilon)]v_F^2\nu(\mu+\epsilon)\tau(\mu+\epsilon) \approx \frac{e^2}{3}[v_F^2\nu(\mu)\tau(\mu)]$$

$$\beta = \frac{e}{3T}\int_{-\infty}^{\infty} d\epsilon\,\epsilon\,[-n_F'(\epsilon)]v_F^2\nu(\mu+\epsilon)\tau(\mu+\epsilon)$$

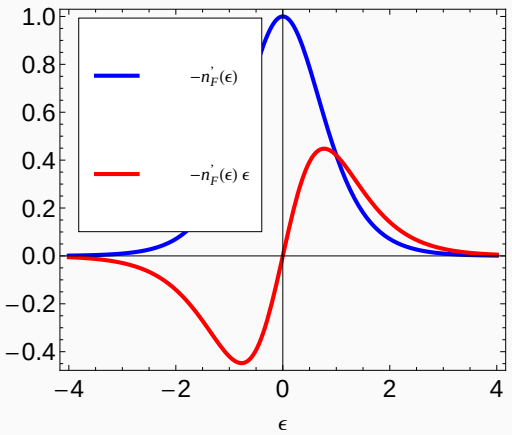

If the product $v_F^2\nu(\mu+\epsilon)\tau(\mu+\epsilon)$ is a smooth function of ϵ, one can expand it:
$v_F^2\nu(\mu+\epsilon)\tau(\mu+\epsilon) \approx v_F^2\nu(\mu)\tau(\mu) + \epsilon\frac{d}{d\mu}[v_F^2\nu(\mu)\tau(\mu)]$
1st term $= 0$ due to oddness, and contributes 2nd.

Arrive at Mott's formula and in normal metals $S = -\frac{\pi^2}{3}\frac{k_B}{e}\frac{k_BT}{\mu} \sim 10^{-2}\,T[\mathrm{K}]\frac{\mu V}{K}$ much smaller than observed in graphene.

Band structure of graphene

Low-energy excitations at two inequivalent K_+, K_- points have a linear dispersion $E_p = \pm\hbar v_F|\mathbf{p}| - \mu$ with $v_F \approx 10^6$ m/s and μ being the chemical potential.

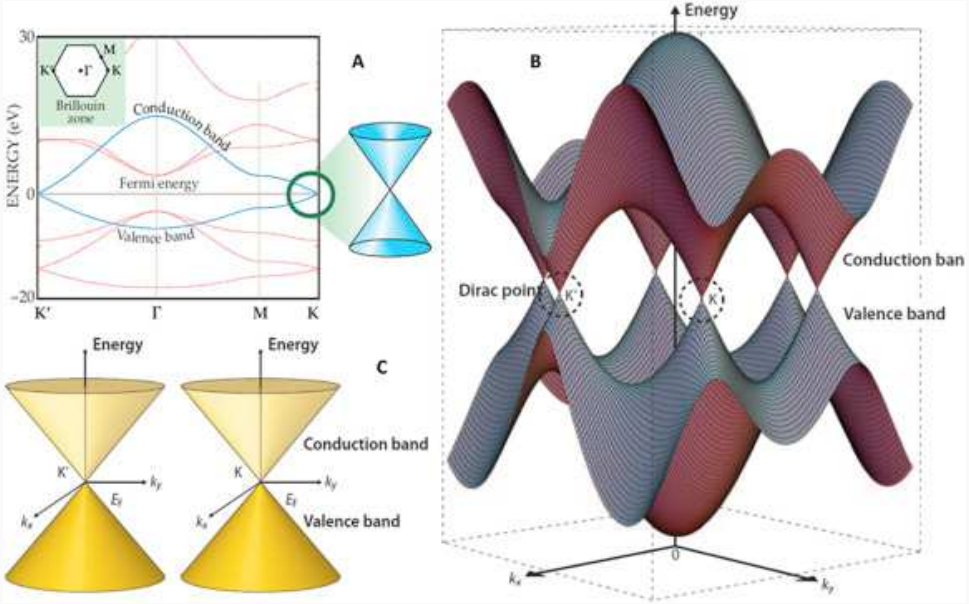

The excitations are described by a pair of two-component spinors $\psi^T_{K,\sigma} = \begin{pmatrix} \psi_{KA\sigma}, \psi_{KB\sigma} \end{pmatrix}$, which are composed of the Bloch states residing (A, B) sublattices with momenta near the two inequivalent points (K_+, K_-) of the Brillouin zone.

The low-energy Hamiltonian

$$H_{K_+} = \sum_{\sigma=\pm1} \int \frac{d^2p}{(2\pi)^2} \psi^\dagger_{K_+\sigma} \begin{pmatrix} 0 & \hbar v_F(p_x - ip_y) \\ \hbar v_F(p_x + ip_y) & 0 \end{pmatrix} \psi_{K_+\sigma},$$

where the momentum $\mathbf{p} = (p_x, p_y)$ is given in a local coordinate system.

Semenoff, PRL 53, 2449 (1984)

Making sublattices inequivalent and graphene gapped

$$H_{K_+} = \sum_{\sigma=\pm 1} \int \frac{d^2p}{(2\pi)^2} \psi^\dagger_{K_+\sigma} \begin{pmatrix} \Delta & \hbar v_F (p_x - i p_y) \\ \hbar v_F (p_x + i p_y) & -\Delta \end{pmatrix} \psi_{K_+\sigma}.$$

The presence of $\Delta \neq 0$ breaks parity $\mathcal{P} : [x \to -x, y \to -y, A \leftrightarrows B]$ and makes the spectrum $E(\mathbf{p}) = \pm\sqrt{\hbar^2 v_F^2 \mathbf{p}^2 + \Delta^2}$ with the mass Δ.

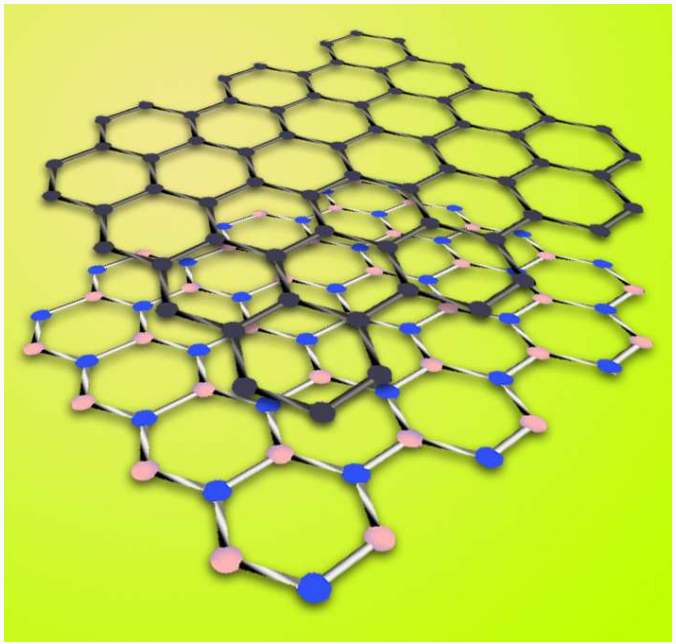

Graphene on top of hexagonal boron nitride (h-BN) – lattice is 1.7% percent larger. Mass (sublattice asymmetry gap) can be induced by interaction with substrate: $2\Delta \sim 350\,\mathrm{K}$.

Making sublattices inequivalent and graphene gapped

$$H_{K_+} = \sum_{\sigma=\pm 1} \int \frac{d^2p}{(2\pi)^2} \psi^\dagger_{K_+\sigma} \begin{pmatrix} \Delta & \hbar v_F(p_x - ip_y) \\ \hbar v_F(p_x + ip_y) & -\Delta \end{pmatrix} \psi_{K_+\sigma}.$$

The presence of $\Delta \neq 0$ breaks parity $\mathcal{P} : [x \to -x, y \to -y, A \leftrightarrows B]$ and makes the spectrum $E(\mathbf{p}) = \pm\sqrt{\hbar^2 v_F^2 \mathbf{p}^2 + \Delta^2}$ with the mass Δ.

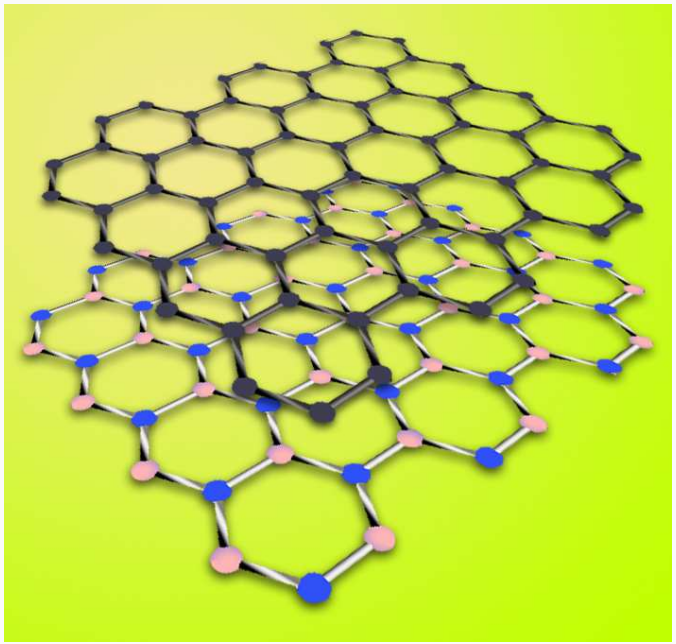

Graphene on top of hexagonal boron nitride (h-BN) – lattice is 1.7% percent larger. Mass (sublattice asymmetry gap) can be induced by interaction with substrate: $2\Delta \sim 350\,\mathrm{K}$.

How the gap affects thermopower?

Quasiparticle scattering near ETT

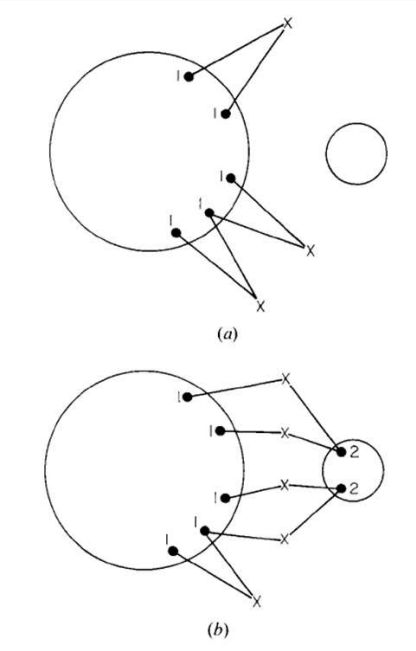

Possible types of electron scattering for a double valley Fermi surface. A.A. Varlamov, V.S. Egorov, and A.V. Pantsulaya, Adv. in Phys. **38**, 469 (1989).

(a) Scattering processes which do not involve the small valley.
(b) Scattering processes where electron gets to the small void, but then gets back to the continuous part of the Fermi surface.

In vicinity of the critical point $\mu = \mu_c$, when the Fermi surface connectivity changes, the quasiparticle relaxation rate $\tau^{-1}(\varepsilon) \equiv \Gamma(\varepsilon)$ also acquires the contribution strongly depending on energy, that generates kinks in conductivity and peaks in thermopower.

Scattering in gapped graphene

Zero mass, $\Delta = 0$

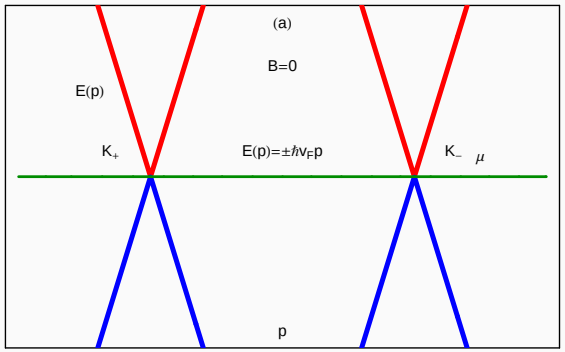

(a) Linear dispersion, $\mu = 0$ as in compensated graphene.

Gapped, $\Delta \neq 0$

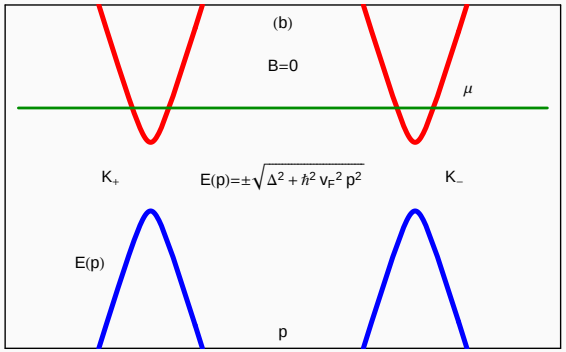

(b) A possible modification of the spectrum by the finite gap Δ. μ is shifted from zero by the gate voltage.

Self-consistent equation for self-energy:

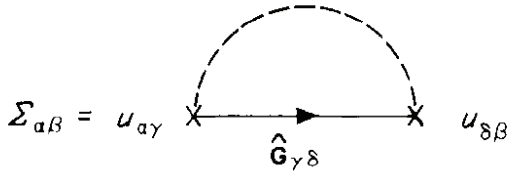

Use relatively long-range potential $\widehat{V}(\mathbf{q})$, i.e. ignore scattering between $\mathbf{K}_{\pm}$, but assume $\widehat{V}(\mathbf{q})$ to be momentum independent for the intra-valley scattering.

Control parameter: $|\Delta| < ?? > |\mu|$

Quasiparticle scattering in graphene

The self-energy $\widehat{\Sigma}(\mathbf{p},\varepsilon_n)=\sum_{i=0}^{3}\sigma_i(\mathbf{p},\varepsilon_n)\widehat{\tau}_i$ Since $\sigma_{1,2}=0$, arrive at the system

$$\left\{\begin{array}{c}\sigma_0^R(\varepsilon)\\ \sigma_3^R(\varepsilon)\end{array}\right\}=\frac{4\hbar}{\pi\tau_0|\mu|}\int_0^W\frac{\left\{\begin{array}{c}\varepsilon+\mu-\sigma_0^R(\varepsilon)\\ \Delta+\sigma_3^R(\varepsilon)\end{array}\right\}\xi d\xi}{\left[\varepsilon+\mu-\sigma_0^R(\varepsilon)\right]^2-\xi^2-[\Delta+\sigma_3^R(\varepsilon)]^2},$$

A new feature, in addition to the usually considered Eq. for σ_0 we also consider Eq. for σ_3 in the gap channel. Then approximately include both channels together:

$$\begin{aligned}\frac{1}{\tau(\varepsilon)}\equiv\Gamma(\varepsilon)&=-\mathrm{Im}\,\sigma_0^R(\varepsilon)-\frac{\Delta}{\varepsilon+\mu}\mathrm{Im}\,\sigma_3^R(\varepsilon)\\ &=\Gamma_0\left[\frac{|\varepsilon+\mu|}{|\mu|}+\frac{\Delta^2}{|\varepsilon+\mu||\mu|}\right]\theta\left[(\varepsilon+\mu)^2-\Delta^2\right].\end{aligned}$$

The relaxation rate acquires the $\theta\left[(\varepsilon+\mu)^2-\Delta^2\right]$ contribution.

Transport coefficients in graphene

Using Kubo formula:

$$\left\{ \begin{array}{c} \sigma \\ \beta \end{array} \right\} = \frac{e^2}{\hbar} \int_{-\infty}^{\infty} \frac{d\varepsilon \mathcal{A}(\varepsilon, \Gamma(\varepsilon), \Delta)}{2T \cosh^2 \frac{\varepsilon}{2T}} \left\{ \begin{array}{c} 1 \\ \varepsilon/(eT) \end{array} \right\},$$

where the function

$$\mathcal{A}(\varepsilon, \Gamma(\varepsilon), \Delta) = \frac{1}{2\pi^2} \left[1 + \frac{(\mu+\varepsilon)^2 - \Delta^2 + \Gamma^2(\varepsilon)}{2|\mu+\varepsilon|\Gamma(\varepsilon)} \times \left(\frac{\pi}{2} - \arctan \frac{\Delta^2 + \Gamma^2(\varepsilon) - (\mu+\varepsilon)^2}{2|\mu+\varepsilon|\Gamma(\varepsilon)} \right) \right].$$

We use regularized scattering rate: $\Gamma^{\text{full}}(\varepsilon) = \Gamma(\varepsilon) + \gamma_0$.

Results

Conductivity $\sigma(\mu)$

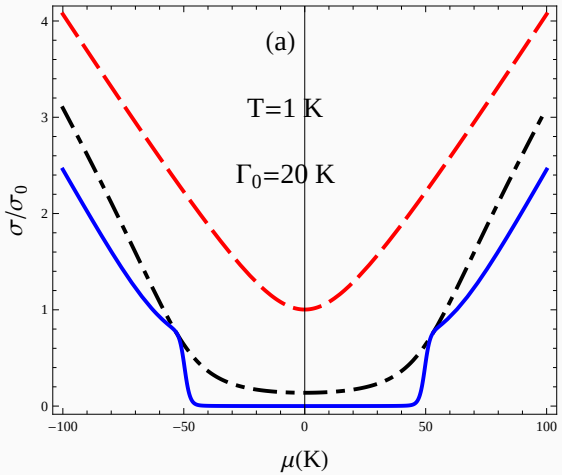

In units $\sigma_0 = \frac{2e^2}{\pi^2\hbar}$

Tm.-el. coefficient $\beta(\mu)$

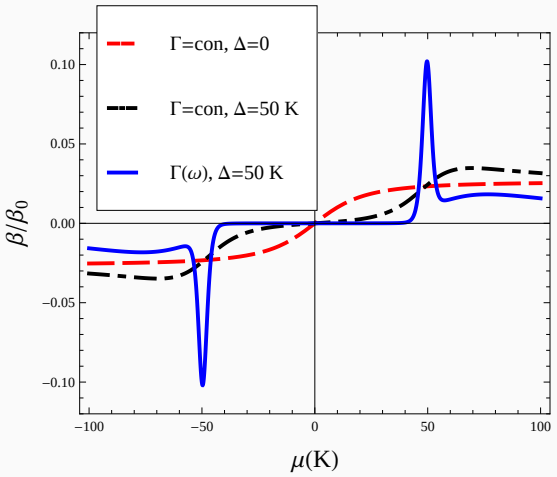

$\beta_0 = k_B e/\hbar,\ T = 1\,K$

Thermopower $S(\mu)$

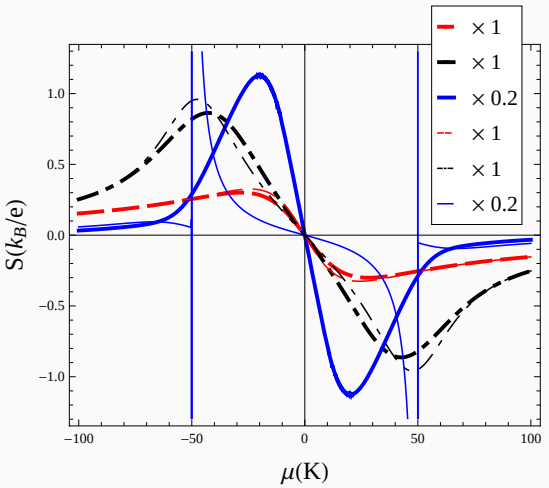

$S_0 = k_B/e,\ T = 5\,K$

— $\Delta = 0$, $\Gamma(\varepsilon) =$ const - reference case: restore normal metal case, $S = -(\pi^2/3e)T/\mu$ in the limit $|\mu| \gg T, \Gamma_0$.

— $\Delta = 50$ K, $\Gamma(\varepsilon) =$ const: E. Gorbar *et al.*, PRB **66**, 045108 (02).

— $\Delta = 50$ K, $\Gamma(\varepsilon)$ - S.G. Sh. and A.A. Varlamov, Phys. Rev. B **86**, 035430 (2012).

Thin lines – from Mott formula.

Conclusions:

- Opening a gap results in appearance of a fingerprint bump of the Seebeck signal when the chemical potential approaches the gap edge.
- Magnitude of the bump can be up 10 times higher than already large value of $S \sim 50 \mu V/K$ at room temperatures observed in graphene.
- Effect is related to a new channel of quasi-particle scattering from impurities with the relaxation time strongly dependent on the energy.
- One can exploit the predicted giant peak of the Seebeck signal as a signature of the gap opening in monolayer graphene.
- Similar phenomenon already observed in bilayer graphene, C.-R. Wang, *et al.*, PRL **107**, 186602 (11).

Nernst - Ettingshausen effect in graphene

Nernst - Ettingshausen effect (1886)

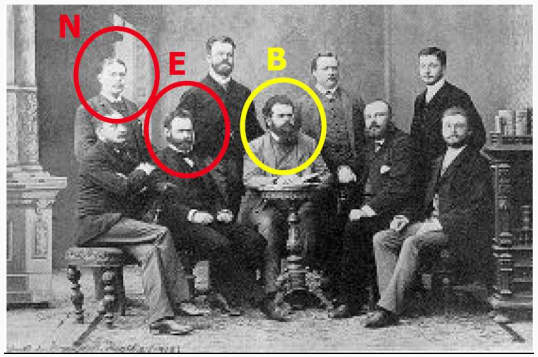

Walther Nernst

1864 - 1941

Nobel Prize in chemistry (1920) in recognition of his work in thermochemistry. Third law of thermodynamics.

Albert von Ettingshausen

1850 - 1932

Nernst effect is the transversal equivalent of the Seebeck effect: $\nabla_x T \rightarrow E_y$

$e_y = -\frac{E_y}{\nabla_x T}\left[\frac{\mu V}{K}\right]$

Energy scale:

$k_B/e \sim 86\,\mu V/K$

Nernst signal measured in the absence of electric current, $j_x = 0$, $j_y = 0$:

$$j_x = \sigma_{xx} E_x + \sigma_{xy} E_y - \beta_{xx} \nabla_x T,$$

$$j_y = \sigma_{yy} E_y + \sigma_{yx} E_x - \beta_{yx} \nabla_x T.$$

2nd NE or Ettingshausen effect: $j_x \rightarrow \nabla_y T$

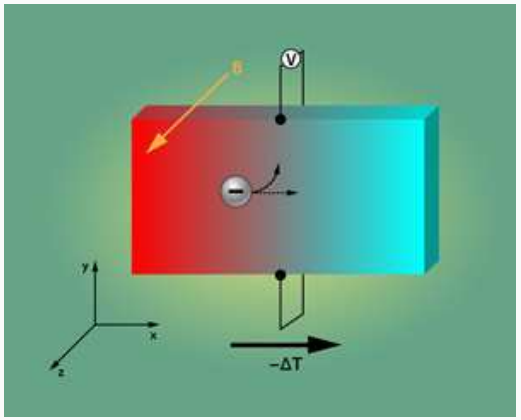

Nernst signal

$e_y(T) = -\frac{\sigma_{xx}\beta_{yx} - \sigma_{yx}\beta_{xx}}{\sigma_{xx}^2 + \sigma_{xy}^2}$

$e_y(T) \approx \frac{\beta_{xy}}{\sigma_{xx}}$

for $\sigma_{xx} \gg |\sigma_{xy}|$

β_{xy} is the thermoelectric coefficient

Also odd and thus sensitive to the details of the electronic structure.

Nernst effect in graphene

We use Mott's formula, but now for β_{ij}. Then the Nernst signal is

$$e_y(T,B) \equiv -\frac{E_y}{\nabla_x T} = -\frac{\pi^2}{3}\frac{T}{e}\frac{\partial \Theta_H}{\partial \mu},$$

where the Hall angle

$$\Theta_H = \arctan\frac{\sigma_{xy}}{\sigma_{xx}}.$$

The large and positive Nernst signal is a fingerprint of the Dirac quasiparticles.
The Nernst signal e_y in $\mu V/K$ as a function of chemical potential.

V.P. Gusynin and S.G. Sh. PRB 73, 245411 (06); I.A. Luk'yanchuk, A.A. Varlamov, and A.V. Kavokin, PRL 107, 016601 (11).

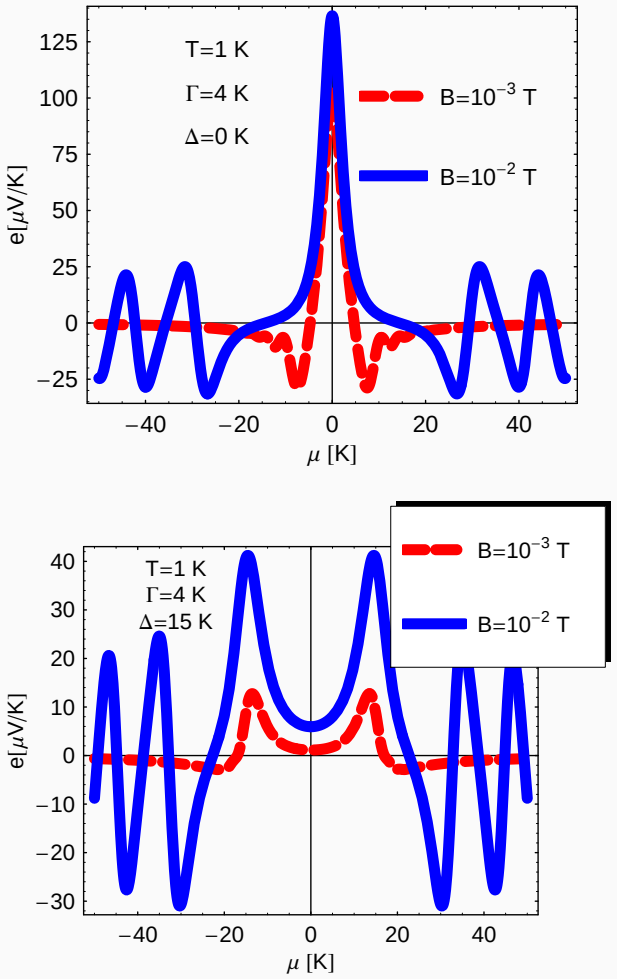

The Nernst signal e_y in $\mu V/K$ as a function of chemical potential

Spin Nernst (SN) effect in silicene

Spin Nernst (SN) effect

SH and SN effects

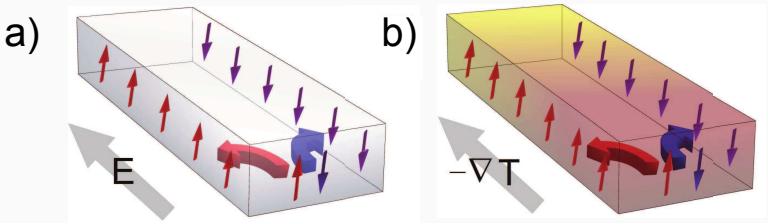

For NE an external magnetic field
$\mathbf{B} \parallel \hat{z} \neq 0$ is required!
Now $\mathbf{B} = 0$, but there is the internal magnetic field or spin-orbit interaction.
SN effect: $\mathbf{j}^s = -\widehat{\beta}^s \boldsymbol{\nabla} T$
with the thermo-spin tensor, $\widehat{\beta}^s$
Purpose is to study SN effect in low-buckled Dirac materials.

Spin Nernst (SN) effect

SH and SN effects

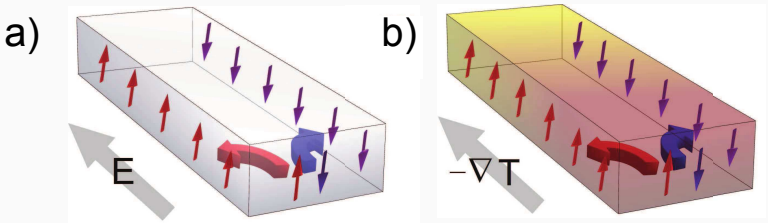

For NE an external magnetic field $\mathbf{B} \parallel \hat{z} \neq 0$ is required!

Now $\mathbf{B} = 0$, but there is the internal magnetic field or spin-orbit interaction.

SN effect: $\mathbf{j}^s = -\widehat{\beta}^s \boldsymbol{\nabla} T$

with the thermo-spin tensor, $\widehat{\beta}^s$

Purpose is to study SN effect in low-buckled Dirac materials.

Spin current subtlety

There is no conservation of spin!

$\frac{\partial S_z}{\partial t} + \boldsymbol{\nabla} \cdot \mathbf{J}_s = \mathcal{T}_z$, where the spin torgue density $\mathcal{T}_z(\mathbf{r}) = \Re e\, \Psi^\dagger(\mathbf{r}) \hat{\tau} \Psi(\mathbf{r})$

with $\hat{\tau} \equiv \frac{d\hat{S}_z}{dt} = \frac{1}{i\hbar}[\hat{S}_z, \hat{H}]$.

When $[\hat{S}_z, \hat{H}] = 0$ the spin torque term is zero and the spin current

$\mathbf{J}_s(\mathbf{r}) = \Re e\, \Psi^\dagger(\mathbf{r}) \frac{1}{2} \left\{ \hat{\mathbf{v}}, \hat{S}_z \right\} \Psi(\mathbf{r})$ with the spinor $\Psi^T = (\psi_\uparrow, \psi_\downarrow)$.

J. Shi, P. Zhang, Di Xiao, Q. Niu, PRL **96**, 076604 (06); P. Zhang, Z. Wang, J. Shi, Di Xiao, and Q. Niu, PRB **77**, 075304 (08).

Low-buckled Dirac materials

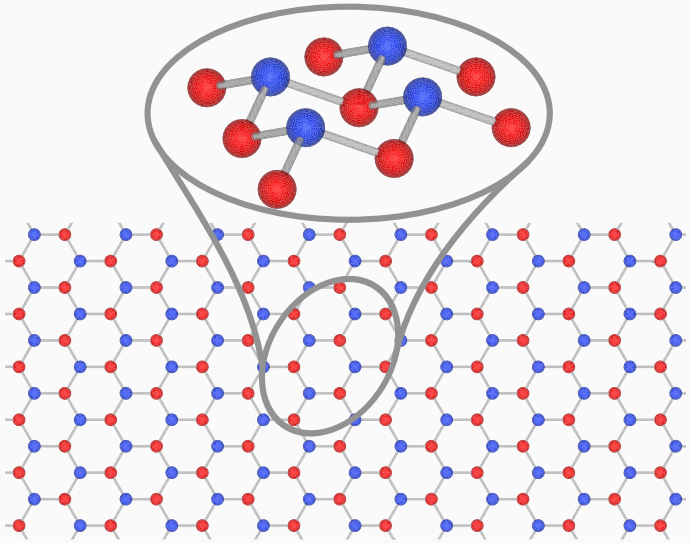

Silicene: vertical distance between sublattices $2d \approx 0.46$Å.
Lattice constant $a = 3.87$Å.
So far grown on Ag and ZrB_2 substrates which are both conductive – no transport measurements as yet.
2D sheets of Ge, Sn, P and Pb atoms (the materials germanene, stanene and phosphorene).

Strong intrinsic spin-orbit interaction in contrast to graphene

$$H_{SO} = i\frac{\Delta_{SO}}{3\sqrt{3}} \sum_{\substack{\langle\langle i,j\rangle\rangle \\ \sigma\sigma'}} c^{\dagger}_{i\sigma}(\boldsymbol{\nu}_{ij}\cdot\boldsymbol{\sigma})_{\sigma\sigma'}c_{j\sigma'}$$

with $\Delta_{SO} \sim 10\,\text{meV}$, $\nu^z_{ij} = \pm 1$.

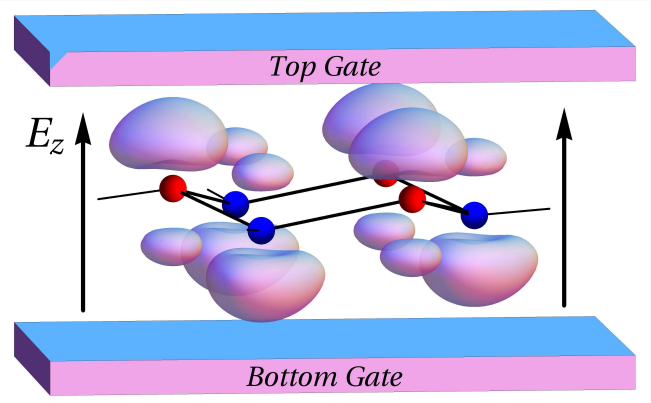

Perpendicular to the plane electric field E_z opens the tunable gap $\Delta_z = E_z d$.
Interplay of two gaps: Δ_{SO} and Δ_z.

Low-energy Hamiltonians and main goals

1. Toy model: two-component Dirac fermions model

$$\mathcal{H} = \hbar v_F (k_x \tau_1 + k_y \tau_2) + \Delta \tau_3 - \mu \tau_0 .$$

The mass Δ breaks TR symmetry. To study off-diagonal part of the TE tensor $\widehat{\beta}$:

$$\mathbf{j} = \widehat{\sigma}\mathbf{E} - \widehat{\beta}\nabla T$$

Low-energy Hamiltonians and main goals

1. Toy model: two-component Dirac fermions model

$$\mathcal{H} = \hbar v_F (k_x \tau_1 + k_y \tau_2) + \Delta \tau_3 - \mu \tau_0 .$$

The mass Δ breaks TR symmetry. To study off-diagonal part of the TE tensor $\widehat{\beta}$:

$$\mathbf{j} = \widehat{\sigma} \mathbf{E} - \widehat{\beta} \nabla T$$

2. Silicene

$$\mathcal{H}_\eta = \sigma_0 \otimes [\hbar v_F (\eta k_x \tau_1 + k_y \tau_2) + \Delta_z \tau_3 - \mu \tau_0] - \eta \Delta_{\mathrm{SO}} \sigma_3 \otimes \tau_3 ,$$

$\boldsymbol{\tau}$ and $\boldsymbol{\sigma}$ – sublattice and spin; $\mathbf{k}$ is measured from the $\mathbf{K}_\eta$ points.
There is a spin $\sigma = \pm$, and valley $\eta = \pm$ dependent gap $\Delta_{\eta\sigma} = \Delta_z - \eta\sigma\Delta_{\mathrm{SO}}$ or mass $\Delta_{\eta\sigma}/v_F^2$, where v_F is the Fermi velocity.
When $\Delta_{\eta\sigma} = 0$ come back to graphene.
TRS is unbroken for any $\Delta_{\eta\sigma}$.
To study off-diagonal part of the thermo-spin tensor $\widehat{\beta}^s$:

$$\mathbf{j}^s = \widehat{\sigma}^{sc} \mathbf{E} - \widehat{\beta}^s \nabla T$$

Anomalous Hall effect

For $B = 0$ equation of motion for $\eta = +$

$$\dot{\mathbf{v}} = \frac{1}{i\hbar}[\mathbf{v}, H] = 2v_F^2 \mathbf{k} \times \boldsymbol{\tau} - \frac{2\Delta}{\hbar}\mathbf{v} \times \mathbf{e}_z, \quad \mathbf{v} = v_F \boldsymbol{\tau}.$$

Here the first term corresponds to Zitterbewegung and the second term corresponds to the Lorentz force due to magnetic field $\mathbf{B}_{eff} \perp$ plane, where $B_{eff} \propto \Delta$. This is related to the Haldane model, Phys. Rev. Lett. **61**, 2015 (1988), also T. Ando, J. Phys. Soc. Jpn. **84**, 114705 (15).
For $T = 0$ the intrinsic (not induced by disorder) AHE

$$\sigma_{xy}^{\eta} = -\frac{e^2 \mathrm{sgn}\,(\eta\Delta)}{4\pi\hbar} \begin{cases} 1, & |\mu| \leq |\Delta|, \\ |\Delta|/|\mu|, & |\mu| > |\Delta|. \end{cases}$$

For $|\mu| > |\Delta|$ the vertex corrections modify the result N.A. Sinitsyn, J.E. Hill, H. Min, J. Sinova, and A.H. MacDonald, PRL **97** 106804 (06). Moreover, the standard diagrammatic approach fails A. Ado, I.A. Dmitriev, P.M. Ostrovsky, and M. Titov, Europhys. Lett. **111**, 37004 (15).

SHE scenario for silicene

Silicene for $B = 0$ TR unbroken $\sigma_{xy} = \sum_{\xi,\sigma=\pm} \xi \sigma_{xy}(\Delta \to \Delta_{\xi\sigma}) = 0$.

SHE scenario for silicene

Silicene for $B = 0$ TR unbroken $\sigma_{xy} = \sum_{\xi,\sigma=\pm} \xi\sigma_{xy}(\Delta \to \Delta_{\xi\sigma}) = 0$.

Kane-Mele scenario of SHE. It occurs due to the presence of two subsystems with $\sigma = \pm$ exhibiting the quantum Hall effect:
$\sigma_{xy}^{S_z} = -\frac{\hbar}{2e} \sum_{\xi,\sigma=\pm} \xi\sigma\sigma_{xy}(\Delta \to \Delta_{\xi\sigma})$.

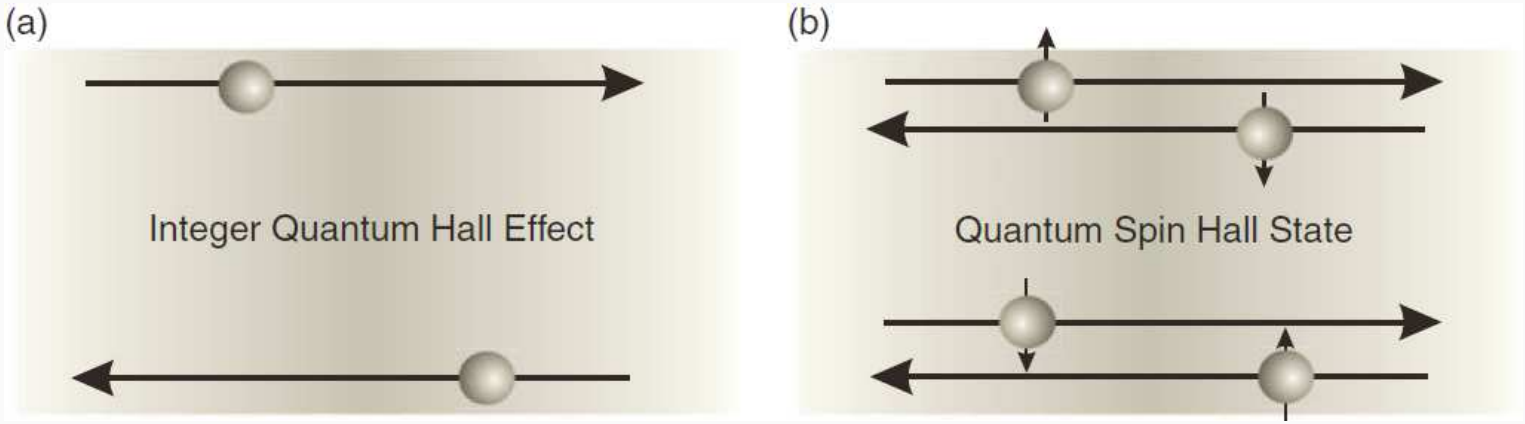

Proposed for graphene in C.L. Kane and E.J. Mele, PRL 95, 226801 (05). For $\Delta_z = 0$
$\sigma_{xy}^{S_z} = -\frac{e}{2\pi} \mathrm{sgn}\,(\Delta_{\mathrm{so}}) \left[\theta(|\Delta_{\mathrm{so}}| - |\mu|) + \frac{|\Delta_{\mathrm{so}}|}{|\mu|}\theta(|\mu| - |\Delta_{\mathrm{so}}|)\right]$ For $|\mu| < |\Delta_{\mathrm{so}}|$ – quantum spin Hall insulator.
$\sigma_{xy}^{S_z}$ is measured in the units of $e/(4\pi)$.

Why interesting physics can be expected

Mott relation for thermoelectric coefficient is not reliable, but can be used for an estimate:

$$\beta_{xy} = -\frac{\pi^2 k_B^2}{3e} T \frac{\partial \sigma_{xy}(\mu, \Delta, T=0)}{\partial \mu}$$

Then the Nernst signal for $\sigma_{xx} \gg |\sigma_{xy}|$ and $|\mu| > |\Delta|$:

$$e_y(T) \approx \frac{\beta_{xy}}{\sigma_{xx}} = -\left(\frac{k_B}{e}\right) \frac{\pi e^2}{12\hbar\sigma_{xx}} \frac{k_B T \Delta \mathrm{sgn}(\mu)}{\mu^2}.$$

The order of magnitude is $e_y(T) \sim k_B/e \sim 86\,\mu V/K$.

Tuning the position of μ by changing the gate voltage one gains from 3 to 4 orders of magnitude in e_y as compared to the normal nonmagnetic metals, where $e_y \sim 10\,nV/K$ per Tesla.

No AHE in silicene, but should be SHE and large spin Nernst effect!

Modified Kubo formula

Problem with the Kubo formula

Consider the usual definition of the thermolectric tensor

$$\tilde{\beta}_{xy} = -\frac{\hbar}{T} \lim_{\omega \to 0} \frac{Q_{xy}^{eq(R)}(\omega)}{\omega},$$

where $Q_{xy}^{eq(R)}$ is the retarded response function of the electric and heat currents.

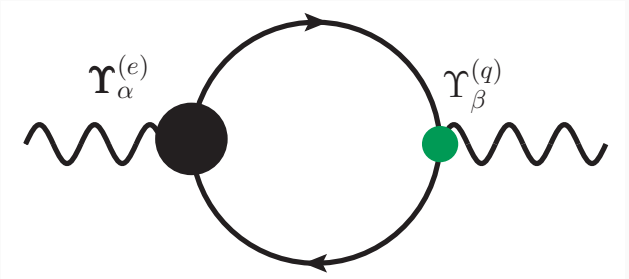

$\Upsilon_{\alpha}^{(e)}$ – electric current vertex [bare $\Upsilon_{\alpha}^{(e)}(\epsilon_n + \Omega_m, \epsilon_n) = -ev_F\tau_\alpha$ and for the full vertex $\Upsilon_{y}^{(e)}$ the contribution $\sim \tau_x$ is also present]; $\Upsilon_{\alpha}^{(q)}$ – heat current vertex.

In the clean case (bare bubble) and in the limit $T \to 0$

$$\tilde{\beta}_{xy} = -\frac{e}{4\pi\hbar T}[\Delta \mathrm{sgn}\,(\mu)\theta(|\mu| - |\Delta|) + \mu \mathrm{sgn}\,(\Delta)\theta(|\Delta| - |\mu|)]$$

diverges!

At $T = 0$ the thermoelectric tensor must become zero: it describes the transport of entropy, which, in accordance with the third law of thermodynamics, becomes zero when $T \to 0$.

Modified Kubo formula

It was shown by Yu.N. Obraztsov, Fiz. Tverd. Tela **6**, 414 (1964) [see also N. R. Cooper, B. I. Halperin, and I. M. Ruzin, PRB **55**, 2344 (1997); T. Qin, Q. Niu, and J. Shi, PRL 107, 236601 (11)] that in the presence of an effective magnetic field, the off-diagonal thermal transport coefficient $\tilde{\beta}_{xy}$ has to be corrected by including of the magnetization M_z term: so that the correct thermoelectric tensor

$$\beta_{xy} = \tilde{\beta}_{xy} + \frac{cM_z}{T},$$

where (V.P. Gusynin, S.G. Sh., and A.A.Varlamov, PRB **90**, 155107 (14).))

$$M_z(B=0) = \frac{e\,\mathrm{sgn}\,(\eta\Delta)\,T}{4\pi\hbar c}\left[\ln\cosh\frac{\mu+|\Delta|}{2k_BT} - \ln\cosh\frac{\mu-|\Delta|}{2k_BT}\right].$$

In the limit $T \to 0$ it cancels out the diverging part of $\tilde{\beta}_{xy}$ and the third law of thermodynamics is restored.

Modified Kubo formula

It was shown by Yu.N. Obraztsov, Fiz. Tverd. Tela **6**, 414 (1964) [see also N. R. Cooper, B. I. Halperin, and I. M. Ruzin, PRB **55**, 2344 (1997); T. Qin, Q. Niu, and J. Shi, PRL 107, 236601 (11)] that in the presence of an effective magnetic field, the off-diagonal thermal transport coefficient $\tilde{\beta}_{xy}$ has to be corrected by including of the magnetization M_z term: so that the correct thermoelectric tensor

$$\beta_{xy} = \tilde{\beta}_{xy} + \frac{cM_z}{T},$$

where (V.P. Gusynin, S.G. Sh., and A.A.Varlamov, PRB **90**, 155107 (14).))

$$M_z(B=0) = \frac{e\,\mathrm{sgn}\,(\eta\Delta)\,T}{4\pi\hbar c}\left[\ln\cosh\frac{\mu+|\Delta|}{2k_BT} - \ln\cosh\frac{\mu-|\Delta|}{2k_BT}\right].$$

In the limit $T \to 0$ it cancels out the diverging part of $\tilde{\beta}_{xy}$ and the third law of thermodynamics is restored.

For silicene the divergence is compensated by the "spin magnetization" $M_z^{S_z} = -\frac{\hbar}{2e}\sum_{\xi,\sigma=\pm}\xi\sigma M_z(\Delta \to \Delta_{\xi\sigma})$, which is nonzero even when the TR symmetry is unbroken. The orbital magnetization $M_z = \sum_{\xi,\sigma=\pm}\xi M_z(\Delta \to \Delta_{\xi\sigma}) = 0$.

Thermo-electric and -spin coefficients:

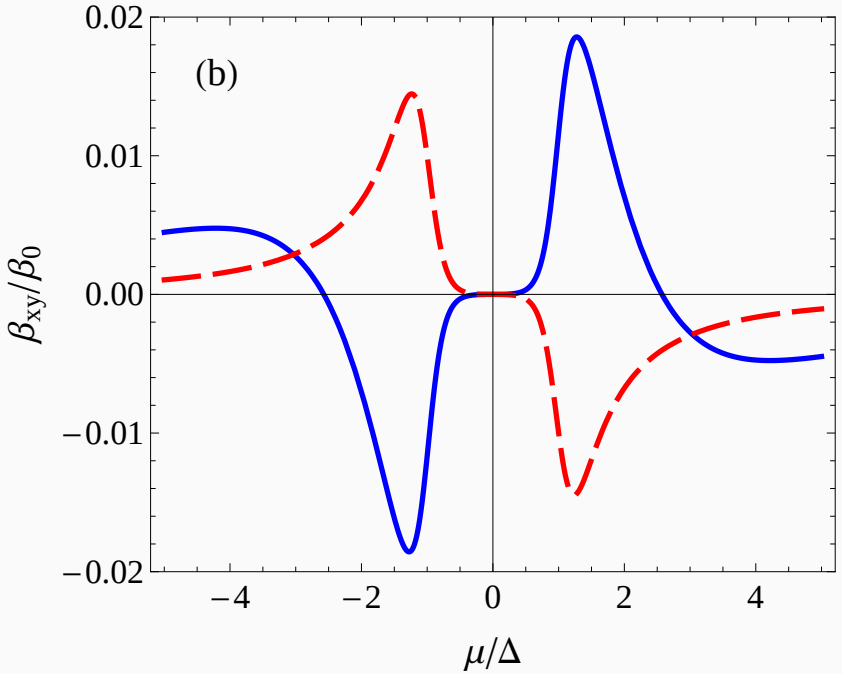

Thermoelectric coefficient $\beta_{xy}(\mu)$ in units of $\beta_0 = k_B e/\hbar$.

Red line — bubble approximation

Blue line — dressed vertex

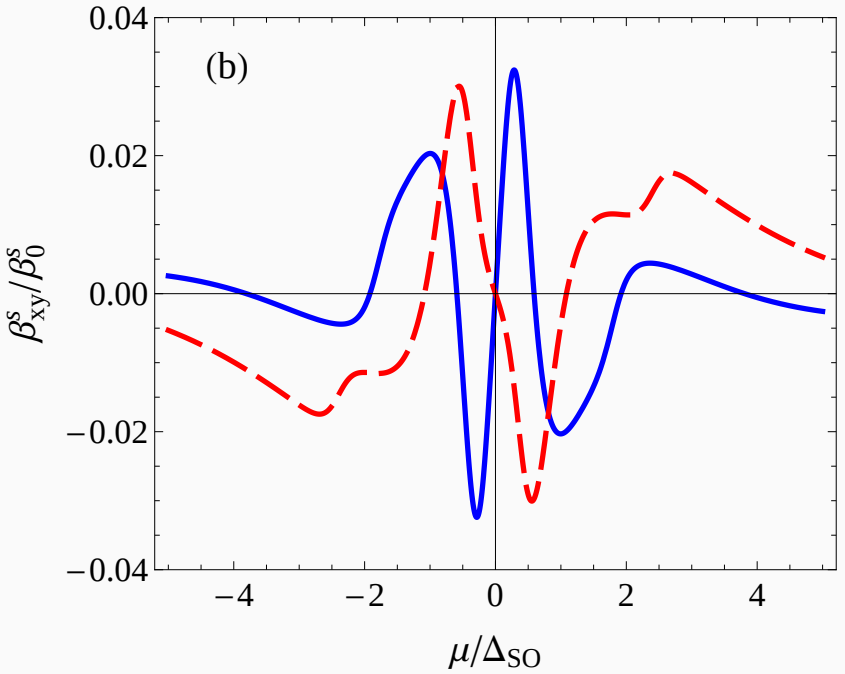

Thermospin coefficient $\beta^{S_z}_{xy}(\mu)$ in units of $\beta^s_0 = k_B/2$.

Crossing $\beta_{xy}(\mu \neq 0) = 0$ is caused by nonmonotonic dependence $\sigma_{xy}(\mu) = 0$ related to the vertex. Other diagrams modify this result.

Results: bare bubble

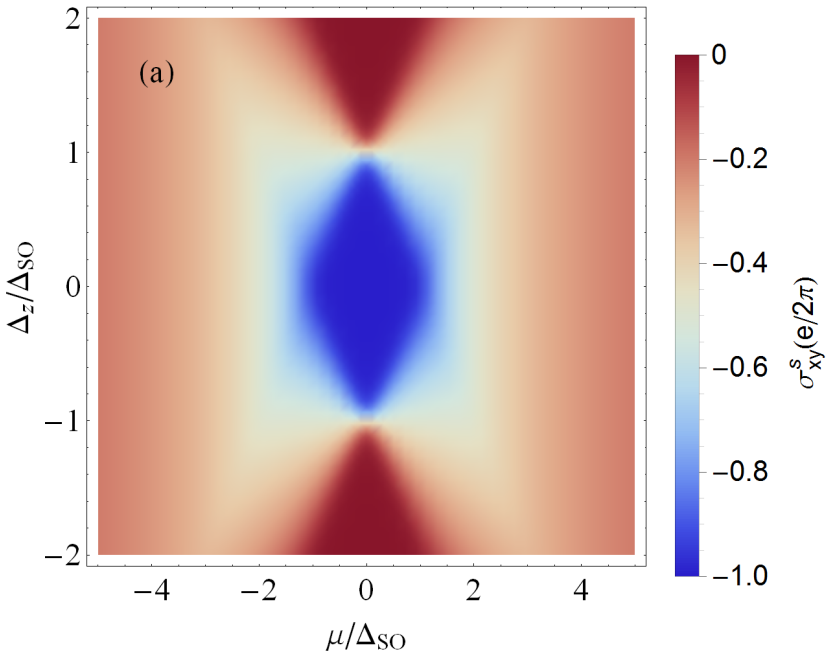

Spin Hall conductivity $\sigma^{S_z}_{xy}(\mu, \Delta_z)$ in units of $\sigma^s_0 = e/(2\pi)$

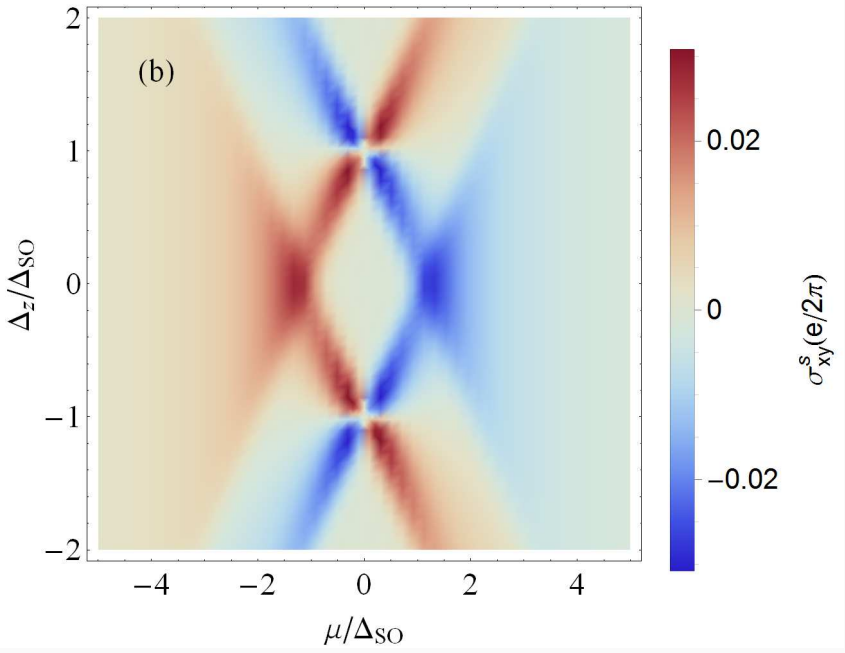

Thermo-spin coefficient $\beta^{S_z}_{xy}(\mu, \Delta_z)$ in units of $\beta^s_0 = k_B/2$

as functions of the chemical potential μ and the sublattice asymmetry gap Δ_z in the units of $\Delta_{SO} > 0$.

Results: vertex

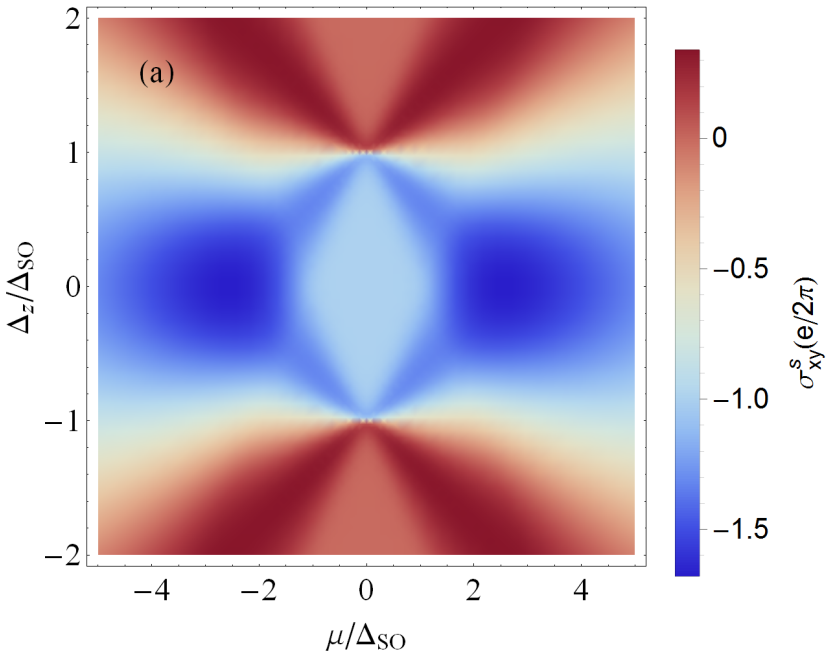

Spin Hall conductivity $\sigma^{S_z}_{xy}(\mu, \Delta_z)$ in units of $\sigma^s_0 = e/(2\pi)$

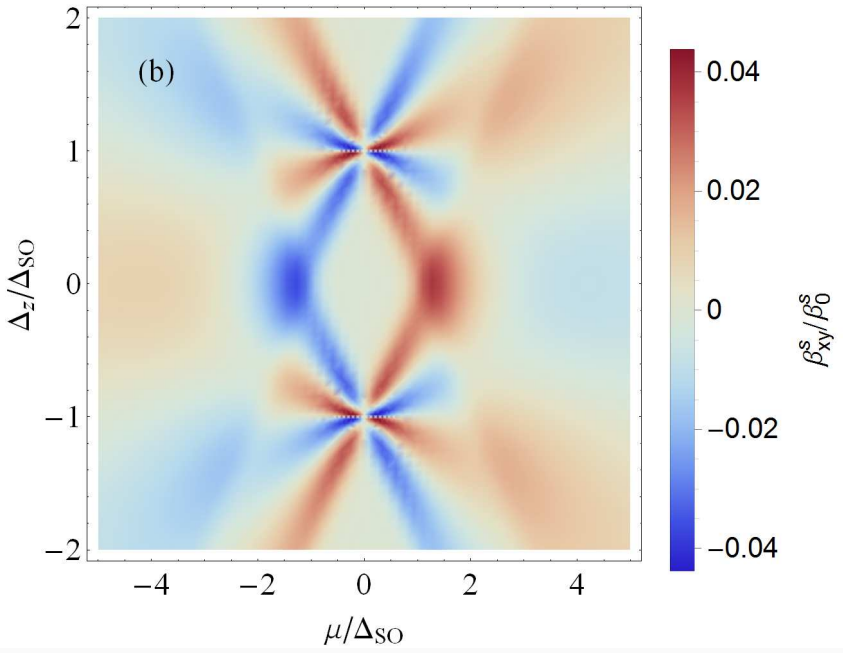

Thermo-spin coefficient $\beta^{S_z}_{xy}(\mu, \Delta_z)$ in units of $\beta^s_0 = k_B/2$

as functions of the chemical potential μ and the sublattice asymmetry gap Δ_z in the units of $\Delta_{SO} > 0$.

Conclusions to Part II

- Spin Nernst effect is strong, so potentially may be observable.
- Illustration how the standard Kubo formula has to be altered by including the effective magnetization leading to the correct off-diagonal thermoelectric coefficient.
- A possibility to distinguish different cases with monotonic and nonmonotonic dependence $\sigma_{xy}(\mu)$ and $\sigma_{xy}^{S_z}(\mu, \Delta_z)$ due to the vertex and other diagrams.

Thank you very much for listening!